Neuro-Oncology Advances

6(1), vdae032, 2024 | https://doi.org/10.1093/noajnl/vdae032 | Advance Access date 2 March 2024

Tumor-treating fields dosimetry in glioblastoma: Insights into treatment planning, optimization, and dose–response relationships

Nikola Mikic, Nichal Gentilal, Fang Cao, Edwin Lok, Eric T. Wong, Matthew Ballo, Martin Glas, Pedro C. Miranda, Axel Thielscher, and Anders R. Korshoej

All author affiliations are listed at the end of the article

Corresponding Authors: Anders R. Korshoej, MD, PhD, Consultant Neurosurgeon, Associate Professor. Aarhus University Hospital, Department of Neurosurgery. Palle Juul-Jensens Boulevard 99. 8200, Aarhus N, Denmark (andekors@rm.dk); Nikola Mikic, MD, Department of Neurosurgery, Aarhus University Hospital, Aarhus, Denmark (nikolanm@gmail.com).

Abstract

Tumor-treating fields (TTFields) are currently a Category 1A treatment recommendation by the US National Comprehensive Cancer Center for patients with newly diagnosed glioblastoma. Although the mechanism of action of TTFields has been partly elucidated, tangible and standardized metrics are lacking to assess antitumor dose and effects of the treatment. This paper outlines and evaluates the current standards and methodologies in the estimation of the TTFields distribution and dose measurement in the brain and highlights the most important principles governing TTFields dosimetry. The focus is on clinical utility to facilitate a practical understanding of these principles and how they can be used to guide treatment. The current evidence for a correlation between TTFields dose, tumor growth, and clinical outcome will be presented and discussed. Furthermore, we will provide perspectives and updated insights into the planning and optimization of TTFields therapy for glioblastoma by reviewing how the dose and thermal effects of TTFields are affected by factors such as tumor location and morphology, peritumoral edema, electrode array position, treatment duration (compliance), array "edge effect," electrical duty cycle, and skull-remodeling surgery. Finally, perspectives are provided on how to optimize the efficacy of future TTFields therapy.

Keywords

computational head modeling | dosimetry | glioblastoma | tumor-treating fields

Tumor-treating fields (TTFields) therapy has been established as an effective adjuvant treatment in newly diagnosed patients with glioblastoma (GBM)[1] and is currently recommended as a category 1A treatment by the American National Comprehensive Cancer Center. TTFields is a low-intensity, intermediate-frequency alternating electric fields used to treat cancer. In GBM, the frequency is 200 kHz and an electric field strength is typically below 5 V/cm in most brain regions. Mechanisms of action (MoA) in TTFields are discussed in depth by Moser et al.[2]

A phase III clinical trial (EF-14) by Stupp et al. confirmed that TTFields improve overall survival (OS) in newly diagnosed patients with GBM (5-year overall survival(OS): 13% versus 5%, $P = .004$)[1] when added to standard therapy without impacting negatively on quality of life.[3] In the recurrent glioblastoma (rGBM) setting, there are conflicting reports on the efficacy of TTFields. A randomized phase III clinical trial (EF-11) including patients with first to fourth recurrence, did not meet the prespecified superiority criteria for OS and PFS endpoints when comparing TTFields monotherapy to best physician's choice chemotherapy (OS was 6.6 and 6.0, $P = .27$).[4] However, subsequent post hoc studies demonstrated significant confounding effects of dexamethasone usage in EF-11, negating the effects of TTFields,[5,6] While a recent meta-analysis found a median overall survival (mOS) of 10.3 months, there is currently no level 1 evidence to support TTFields treatment of rGBM.[7] In addition, TTFields are used for mesothelioma[8] and are being investigated as an adjuvant treatment for a number of extracranial cancers, including ovarian cancer, metastatic non-small-cell lung cancer, and pancreatic cancer.[9–12] Although

the preliminary results of phase III clinical trial for ovarian cancer (EF-28, NCT03940196) reportedly failed to show an improved OS with the addition of TTFields to cytotoxic chemotherapies (12.2 months vs. 11.9 months), the full report has not been published yet and subgroup analyses are still ongoing. However, the clinical phase III (LUNAR) trial for metastatic non-small-cell lung cancer concluded significantly improved OS with the addition of TTFields therapy to immunochemotherapy (13.2 vs. 9.9 months, $P = .037$).[13] Finally, the results of the phase III clinical trial for pancreatic cancer (EF-27, NCT03377491) are pending and the trial is expected to complete accrual at the end of 2024.

Despite the well-established clinical evidence, appropriate dosimetry and its correlation with patient outcome remains controversial.

This paper explores definitions of TTFields dose and assesses the current evidence of a dose–response relationship. Moreover, the review examines and evaluates the factors influencing TTFields dose and efficacy and discusses the most recent methodological developments in the computation of TTFields, including heat effect and thermal modeling.

Determination and Importance of TTFields Dose

In vivo and in vitro studies indicate that the antimitotic effects of TTFields depend on multiple factors. The tumor growth rate decreased with higher field intensities (V/cm), longer treatment duration, optimum frequency (200 kHz for GBM), and the direction of the applied field relative to the direction of mitosis.[14–17] The multiple factors complicate a definition of and consensus on optimal dosimetry in TTFields therapy. However, it becomes clear when implementing these factors into the clinical setting that the frequency is fixed and predetermined for each indication and thus less relevant for individual treatment optimization. Similarly, the highest compliance with respect to quality of life is preferred as retrospective studies indicate that treatment duration and patient compliance are positively associated with improved clinical outcomes.[18,19] This leaves the transducer array placement (direction of the applied field) and field intensity as potential parameters that can be optimized on an individual basis.

Previous studies on dosimetry have focused mainly on computational methods to calculate the field distribution, using the field direction and intensity as surrogate metrics of antitumor dose (Figure 1) in accordance with preclinical observations.[20,21] Computational methods have shed light on several intricacies of TTFields therapy, but they are highly technical, time-consuming, and mainly based on research methodologies unsuitable for clinical implementation. However, recent studies have used a multiparametric and possibly more accurate definition of dose, which will be reviewed in detail. Ideally, clinical treatment planning and optimization would be based on tangible and validated TTFields dosimetry software, similar to well-known dose-planning software in radiotherapy.

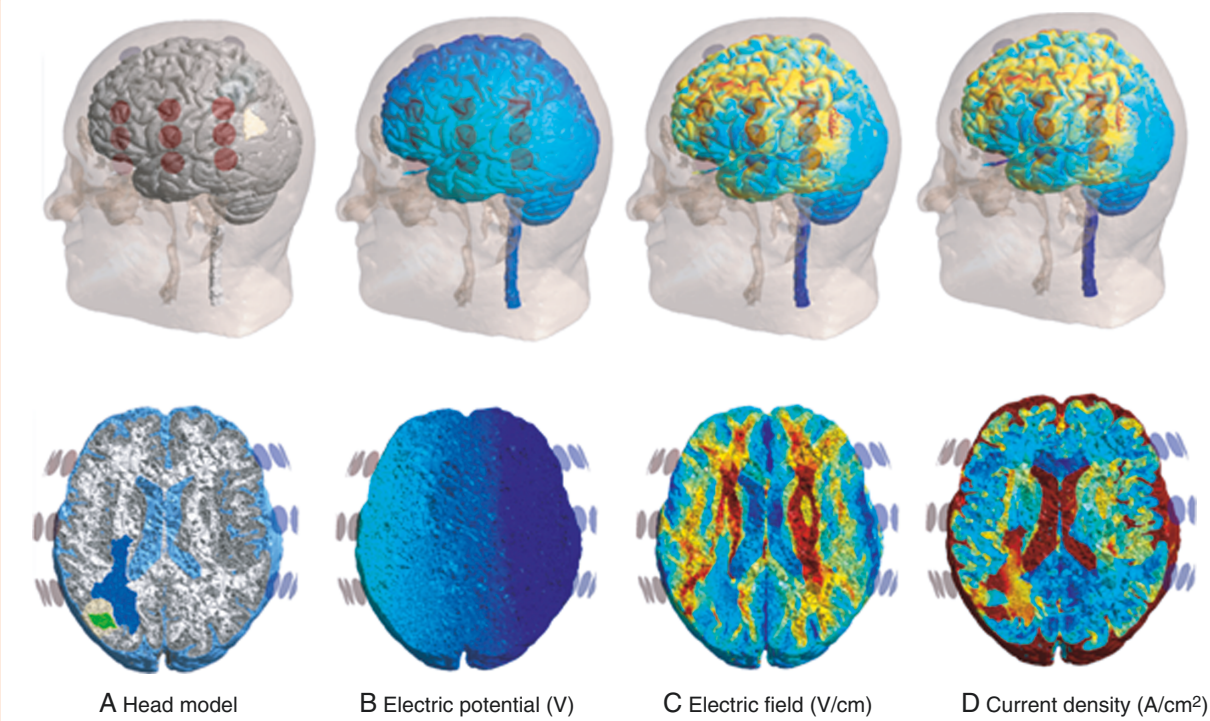

Figure 1. Examples of various methods to show field distribution. The top row visualizes the transducer array clearly and bottom (A) Axial view of the head model before calculations are performed. Blue corresponds to peritumoral edema, green, and yellow to tumor and necrosis, respectively. Axial view of the calculated (B) electric potential, (C) field distribution (V/cm), and (D) current density (A/cm^2).

NovoTAL—The Current Method of Transducer Array Layout Planning

Personalized array layouts for clinical treatment are produced using the commercial software NovoTAL (Novocure, LLC), approved by the US Food and Drug Administration. NovoTAL is designed to maximize the intensity of TTFields in the tumor, but the NovoTal method has not been validated and the clinical value of the method thus still needs to be determined. The software is based on a graphical user interface allowing the user to enter morphometric measurements such as the patient's head size, tumor size, and tumor position based on MR images.[22] The morphometric measurements are processed by the software and matched topographically to a library of 72 precalculated field distributions based on different array layouts and a computational model of a healthy subject (courtesy of Novocure, Ltd.). The software selects the layout producing the highest average field intensity in the tumor region. Although this approach is clinically feasible, the generic and generalized calculation based on a computational model of an idealized brain may constitute a significant pitfall concerning accuracy and reliability. This approach does not account for specific individual anatomic characteristics such as the exact morphology and composition of the tumor, presence of edema or resection cavities, and skull thickness. The software produces an outline of the layout on an animated phantom (Figure 2), but the actual resulting field distribution is not shown. This limits critical interpretation and evaluation of the result.

Correlation Between TTFields Dose and Clinical Outcome

Post hoc analyses of the EF-14[1] trial indicate a positive association between clinical outcome and the exposure time and field intensity-based metrics based on the randomized trial cohort by Toms et al.[18] In their analysis, OS improved in a stepwise fashion from a median overall survival (mOS)

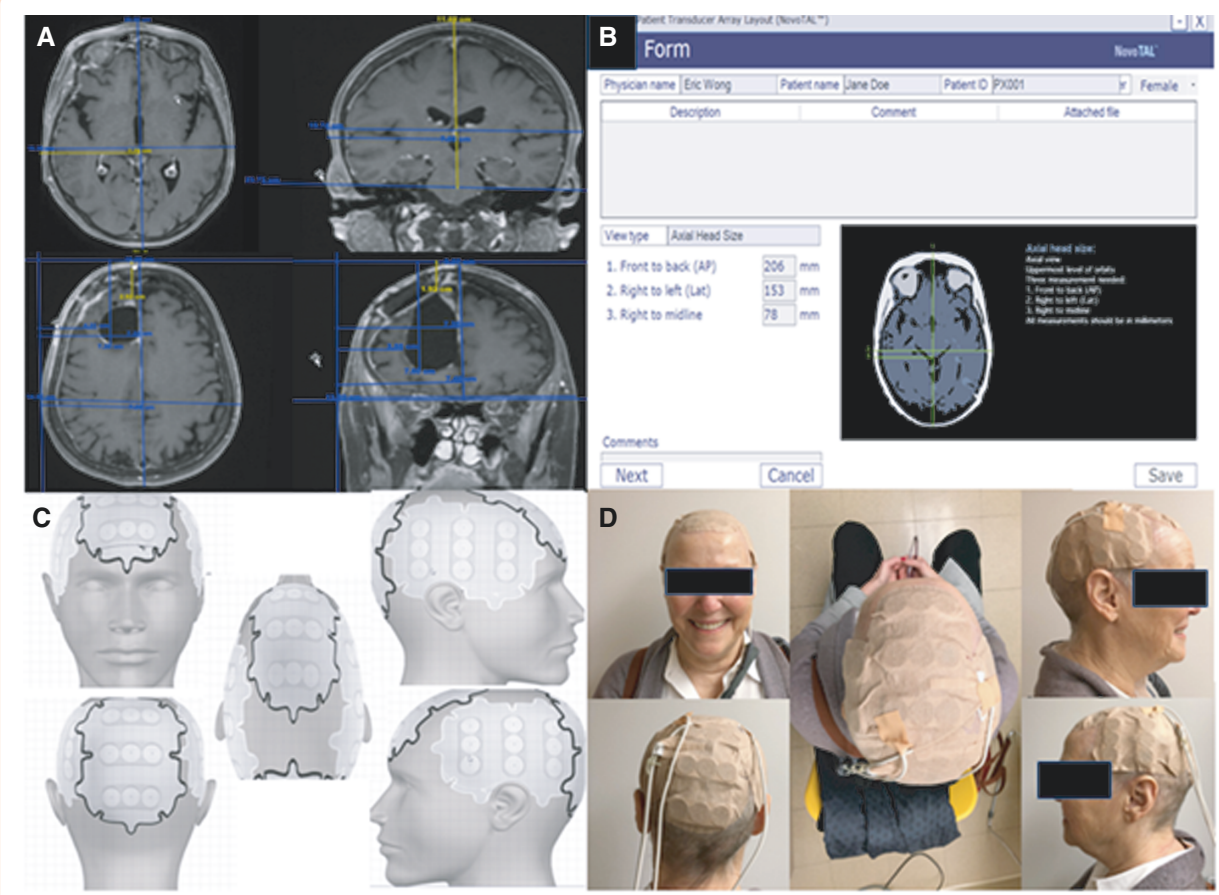

Figure 2. NovoTAL array mapping for the Tumor-Treating Fields device Optune. (A) The patient's head size was measured on MRI DICOM images in the anterior-posterior and right-left directions in the axial view, and in the rostral-caudal and right-left directions in the coronal view (upper panels). The residual tumor adjacent to the resection cavity was also measured in the axial and coronal views (lower panels). (B) The measurements were then entered into the NovoTAL software. (C) The array map was generated by the software in the anterior, right, left, and posterior positions (clockwise), as well as the top view showing all 4 arrays (center). (D) The transducer arrays were then applied to the patient as seen in the anterior, right, left, and posterior positions (clockwise), and in the top view showing all 4 arrays (center).

of 18 months with an average treatment compliance of 50%–60% compared to 19.9 months with a compliance of 60%–70%, 21.7 months with a compliance of 70%–80%, 21.5 months with a compliance of 80%–90%, and 24.9 months with a treatment compliance >90%.[18]

Ballo et al. used MRI scans of patients in the EF-14 trial to retrospectively calculate the patient-specific TTFields dose to the tumor bed and demonstrated a correlation between TTFields dose and patient survival.[23] The analyses were based on calculations of 2 separate dose metrics, the field intensity (E) and the power loss density (PLD,), at any given volume element in the mesh template. The PLD represents the energy per unit of time deposited by TTFields within the region of interest and is defined as

$$\mathrm{PLD} = \frac{1}{2}\sigma E^2. \quad (1)$$

where σ is tissue conductivity (S/cm), and E is the magnitude of the electric field (V/cm). The metric is comparable to a commonly used dose metric in radiation therapy and represents the rate at which energy is imparted by the field to the tissue. As discussed above, the advantage of field intensity is that it is directly correlated with preclinical observations.

As TTFields therapy was delivered by 2 pairs of arrays, Ballo et al. defined the conservative dose estimate of local minimum PLD (LMiPD) and the local minimum field intensity (LMiFI), corresponding to the lower of the 2 respective values at any given point.

For each of these measures, the average dose in the tumor bed was calculated, defined as all volume elements in the mesh containing the enhancing tumor and a 3-mm boundary zone around the enhancing tumor, necrotic regions, and the resection cavity. These metrics were used to determine the collective average dose in the region of interest ie, the average LMiFI and LMiPD, respectively.

The analysis of the patients in the EF-14 study undergoing TTFields therapy was based on LMiFI and LMiPD while considering compliance and prognostic factors (age, sex, MGMT status, KPS, resection status, and tumor location). The analysis demonstrated statistically improved patient survival when the average LMiFI was ≥1.06 V/cm. The median survival was 24.3 months (95% CI: 19.6, 33.0) when the average LMiFI in the tumor bed was >1.06 V/cm versus 21.6 months (95% CI: 18.7, 24.1) in the group with a field intensity of less than 1.06 V/cm[24]. As expected, comparable results were seen when the average LMiPD was ≥1.15 W/cm^3 as the 2 metrics are closely related. Since LMiFI and LMiPD can predict patient outcomes, both represent relevant TTFields dose metrics. PLD is potentially of higher clinical relevance as it is comparable to radiation dose, which is a well-established and accepted metric in radiation therapy.

To account for patient compliance and treatment exposure time, Ballo et al. introduced the more comprehensive dose definition "local minimum dose density" (LMiDD). The LMiDD is defined as the product of PLD and the average fraction of patient compliance during the first 6 months of therapy (U), ie,

$$\mathrm{LMiDD} = \frac{1}{2}\sigma E^2 \cdot U \quad (2)$$

Correlation Between Dose and Progression Patterns

The topographical correlation between TTFields dose and radiological progression patterns was investigated by Glas et al. (2021).[24] Using MRI scans from the EF-14[1] patient cohort, the investigators retrospectively calculated the individual TTFields distribution using patient-specific deformable co-registration to accurately define a computational model including regions of pathology.[24] LMiDD was used as the dose metric (Equation 2). MRI scans obtained at the time of recurrence were registered together with the calculated dose distributions to assess the dose in recurring tumor regions. The authors found that 51% of distal progressions (new lesion not connected with the baseline lesion) in the control group occurred within 2 cm of the primary tumor boundary; this was only the case for 25% of the distal progressions in patients undergoing TTFields therapy. On a macroscopic level, TTFields thus seem to suppress local tumors and distal recurrence becomes the norm. In the analysis by Glas et al., progression-free areas of the normal brain consistently received a higher dose of TTFields than similar areas of the normal brain developing a visible tumor. This result supports the assumption of a dose–response relationship of TTFields indicating that higher fields might prevent or stall tumor progression. Furthermore, there may be a need for continuous adaptation of the individual array layout to ensure global brain coverage with sufficient dose levels to reduce the overall recurrence rate.

Technical Aspects of TTFields Dosimetry Using Computational Models

The following sections describe the basic steps of the calculation process. Further details can be found in Supplementary Material 1.

Step 1—Creation of Head Models—the Framework for Computation

TTFields models are mainly based on semi-automatic segmentation of head MR images constructed into separate anatomical compartments, including scalp, compact bone, spongy bone, cerebrospinal fluid (CSF) space, white matter (WM), gray matter, large blood vessels, eyes, and extraocular muscles (15–18). Among the many algorithms available for tissue segmentation,[25–27] the complete head anatomy reconstruction method provides the most accurate automatic segmentations.[28]

In general, 2 different approaches can be adopted when creating head models for TTFields (Figure 3). In the first approach, the basic model is based on MR images of a healthy person adding an artificial virtual tumor. This approach is highly flexible, allowing investigation of several parameters eg, tumor size, shape, and position, but does not account for anatomic variability and complexity of real patient characteristics. The second approach uses patient MR images to create an individual patient-specific model. This approach is more

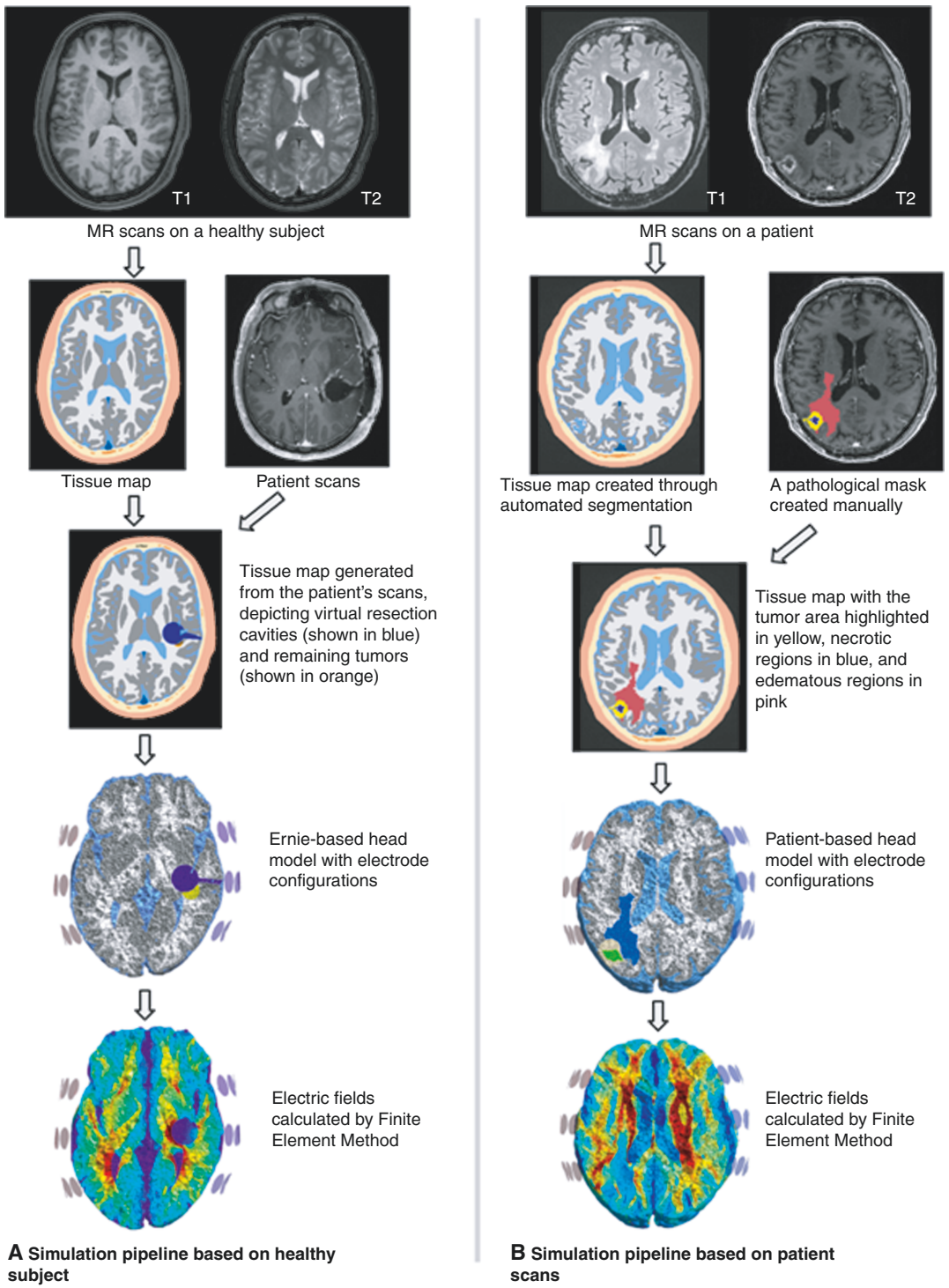

Figure 3. Two different examples of the workflow to create a computational head model. (A) is based on a healthy subject's MR images and afterward virtual pathology is inserted manually based on a patient's postoperative MRI scans and (B) is based on a real patient's MRIs. Specifically, (A) The complete head anatomy reconstruction method segmentation was performed on the T1 and T2 weighted images based on a healthy subject (top image). Postoperative T1 weighted, axial, MRI showing the patients' resection cavity and contrast-enhancing residual tumor (second image from the top to the right). The features of the postoperative MRI are manually imposed (resection cavity and surgical access corridor [blue] and residual tumor [yellow]) on the computational head model. Next, was the finite element mesh generation using the optimized mesh settings for the TTFields. Two 3 × 3 transducer arrays with electrodes of a height of 1 mm and diameter of 2 cm were used. The center-to-center distance between the electrodes was 45 × 22 mm. The electric fields were calculated using FEM. (B) The patient's MRI is used both for the basic model but also for the pathology. The complete head anatomy reconstruction method segmentation was performed on the T1 and T2 weighted images based of a patient's MRI. Manual correction is needed to correctly identify the pathological areas (edema, tumor, and resection cavity). Finite element mesh generation and application of transducer arrays. Electric field is calculated using FEM.

accurate but requires considerable and time-consuming editing. Moreover, it is less flexible for exploratory investigations.

As mentioned, complete head anatomy reconstruction method is fast and accurate in segmenting MRI data in healthy subjects but is unable to do it accurately in actual GBM patient's MRI datasets where pathological tissue is present. The initial segmentation of tumor tissue will likely have inaccuracies and therefore require manual editing to ensure correct labeling of each voxel within the pathological tissue and thus ensure the overall high quality of the model. This process requires time to overcome these complex manipulations to ensure accurate computation of TTFields in the brain.

A consistently high quality of MRI data is crucial to avoid severe segmentation errors. Future studies would thus strongly benefit from optimized and standardized MRI sequences.[28]

Step 2—Assignment, Estimation, and Validity of Electric Properties

After segmentation, values are assigned to each physical parameter in the relevant equations eg, electric and thermal conductivity while the influence of electric permittivity is negligible.[20] The most widely adopted approach is to assume constant, homogeneous, and isotropic parameter values in each segmented volume (Figure 4A) with mean estimates based on previous in vivo and in vitro measurements (Supplementary Material 2). However, this approach does not account for intra- and inter-subject parameter variations or the complex tissue microstructure. TTFields intensity distribution (at 200 kHz) may vary up to 68% with homogenous conductivity.[20]

More complex methods are needed to account for the structural heterogeneity in the brain and tumor regions,

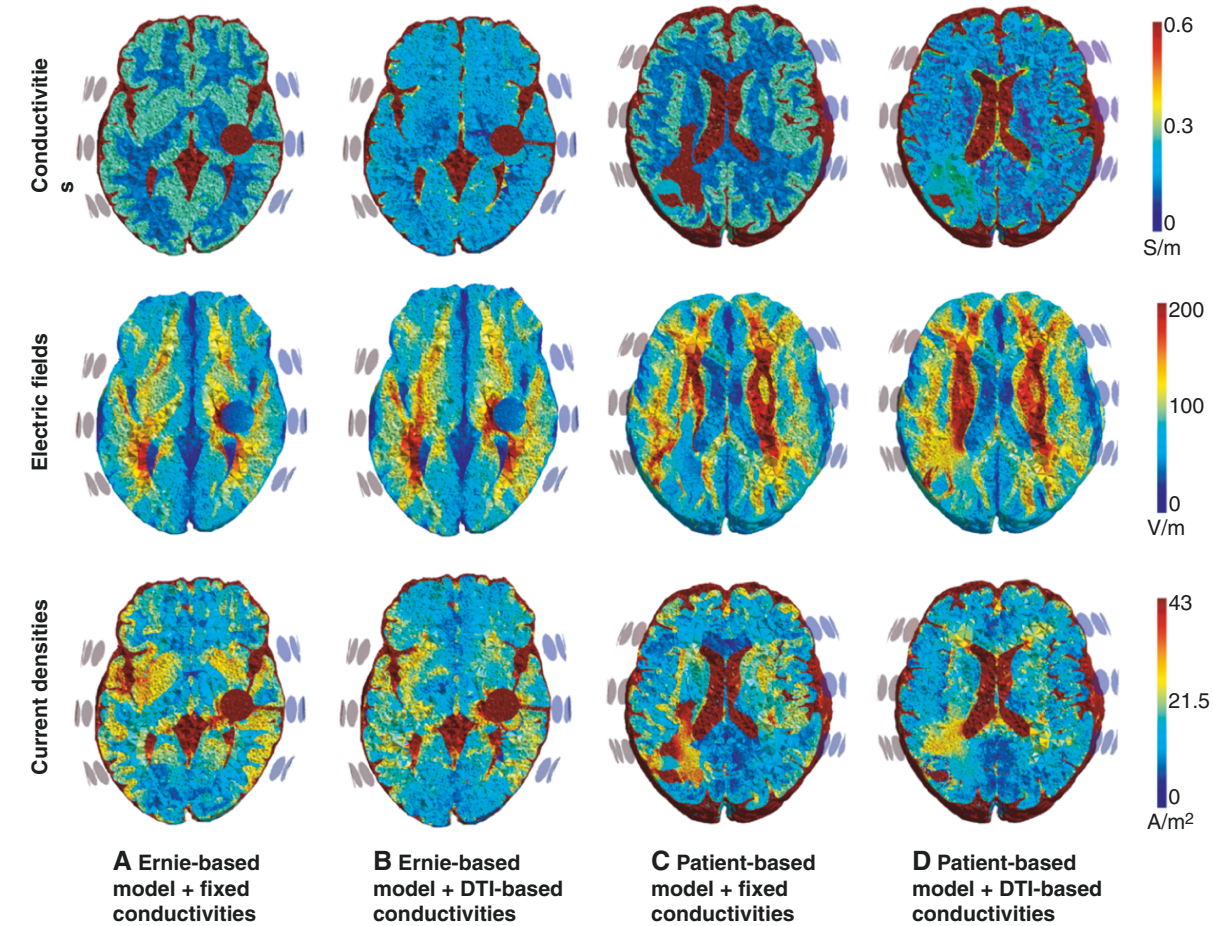

Figure 4. Shows the different methods that can be used to assign tissue conductivity values. The 3 axial views from top to bottom show conductivity, electric field intensity, and current density. The key differentiation lies in the conductive values—whether they are assigned based on median isotropic (ie, "fixed") values, or whether they are calculated specifically for the individual MRI using diffusion tensor imaging (DTI). In the figures with DTI-based conductivities, the conductive values were determined by direct mapping from DTI to conductivity anisotropy, under the assumption of a linear relationship between water and ion diffusivity. It allows for more personalized conductivity calculations that may reflect intra-subject variations more accurately. (A) and (B) head model is based on Figure 3A, ie, healthy subject MRI as baseline and afterward manually added the pathology of a resection cavity, tumor remnant, and surgical access corridor. The main difference is for (A) "fixed" values have been used and (B) DTI has been used for the healthy tissue and "fixed" values have been used for the pathology. This changes the field distribution slightly, mainly due to anisotropy as further explained in figure 5. (C) and (D) head models are based on Figure 3B ie, a patient's preoperative DTI MRI. The main difference between (C) and (D) are "fixed" conductive values and individually calculated by DTI. Note how especially the peritumoral edema affects the field distribution differently in the 2 methods.

such as water-content-based electric properties tomography (wEPT)[29] and diffusion tensor imaging, to estimate conductivity in each voxel in individual patients (Figure 4D).[30–32] The direct mapping from diffusion tensor imaging to anisotropic electric conductivity has been used in this paper (Figure 4D), assuming a linear relationship between water and ion diffusivity. The generated individual patient maps highlighted considerable intra-subject tissue variations (29) and revealed a directional variability in conductivity at every point in the head (anisotropy).[33] The difference between isotropy and anisotropy is shown in Figure 4. Although these approaches are promising to improve model accuracy, further validation is needed.[29,32]

Step 3—Field Calculation

The third and last step involves calculation of the electric potential, which is done by the finite element method (FEM)[21,34,35] using simulation software. The SimNIBS is a well-recognized FEM-based open-source software package well-suited for simulating TTFields.[25] Electrode array models are added (Figure 3) and as all electrodes of an array are fed by the same channel of the stimulator, they are modeled to receive the same stimulation voltage. After using FEM to solve the electric potential, the electric fields are calculated as the gradient of the electric potential and then the current density is finally computed from the electric field using Ohm's law. The electric field values and the current densities are scaled to ensure a total peak-to-peak amplitude for each array pair corresponding to the current level used for clinical TTFields therapy by the Optune device. The implementation of FEM has been described by Saturnino et al.[26]

Essential Findings From Computational Modeling Impacting Dose and Distribution of TTFields

This section highlights some of the most important findings in current dosimetry studies and discusses basic rules to assist treatment planning.

Influence of Electric Conductivity and Tissue Anisotropy

Generally, higher fields will be induced in low-conductivity tissues such as the WM regions, or low-conductivity regions of the tumor. Conversely, low field intensities are induced in high-conductivity regions such as the CSF space. Due to tissue anisotropy, fields will be higher in fiber tracts running orthogonally to the field direction eg, the corpus callosum when TTFields are applied in the anterior-posterior (A/P; Figure 5D, A/P) direction and the medial fibers facing the lateral ventricles when in the left-right (L/R; Figure 5D, L/R) direction.

Current Shunting Through the CSF

As the induced currents will follow the path of least resistance, strong currents will be shunted through the CSF, including the subarachnoid space, sulci, resection cavities, and the ventricular system.[34] Thus, high fields will often occur in the vicinity of a resection cavity, in sulcal fundi, and in periventricular regions, where strong currents are forced through low-conductivity neighboring regions.

Furthermore, the field lines will generally run directly from one array toward the other, although the complex anatomy of the brain causes significant deviations from this in some regions. However, this principle is important to understand eg, to predict which regions surrounding a CSF-filled resection cavity will be affected the most. In a CSF-filled cavity, which has isotropic uniform high-conductivity values, currents will flow between the electrodes and cause strong fields in the part of the resection border, which is perpendicular to current flow. Conversely, the parts that are parallel to the current flow experience low fields and will be less affected. In short, currents will generate high fields when encountered by opposing resistive tissue (Figure 5).

Furthermore, the amount of the CSF within the subarachnoid space will influence electric field penetration into the brain parenchyma. The higher the conductivity through the CSF, the more current will be shunted tangentially, which effectively shields the brain and tumor from TTFields exposure. This may be seen in eg, brain atrophy or in the case of a subdural hygroma.[36]

Peritumoral Edema

Similar to current shunting in CSF spaces, peritumoral edema has been shown to significantly reduce the electric field strength focally in the tumor due to the increased conductivity in edematous region(s). Since edema is highly conductive compared to WM,[37] it tends to shunt the current around the tumor, potentially decreasing the efficacy of TTFields therapy. Computational modeling has indicated that edema decreases field strength in the tumor by 26% on average and potentially up to 52%.[38] Similar results were reported[37] and confirmed in computational studies,[39] where different conductive values and sizes were assigned to edema and compared to controls. The latter study concluded that the larger the edema-to-tumor ratio and the higher the conductivity of edema, the more field strength will be diminished in the tumor.

The conclusions of these studies indicate that edema may be considered a compromising factor reducing the efficacy of TTFields in clinical practice. Future computational models would probably benefit from being individualized to account for the change in field distribution caused by edema, particularly in the pathological region close to the tumor.

Tumor Location and Morphology

Although the electric field does not decrease linearly throughout the brain, tumors located close to the electric source will be exposed to the highest field intensities as current density is highest in these regions.[36] However, high electric fields might still be observed in deeply seated tumors composed of low-conductive components, and hot spots may be observed in varying WM regions. Therefore, it is difficult to predict who will benefit from TTFields therapy without computational modeling of the electric fields. The

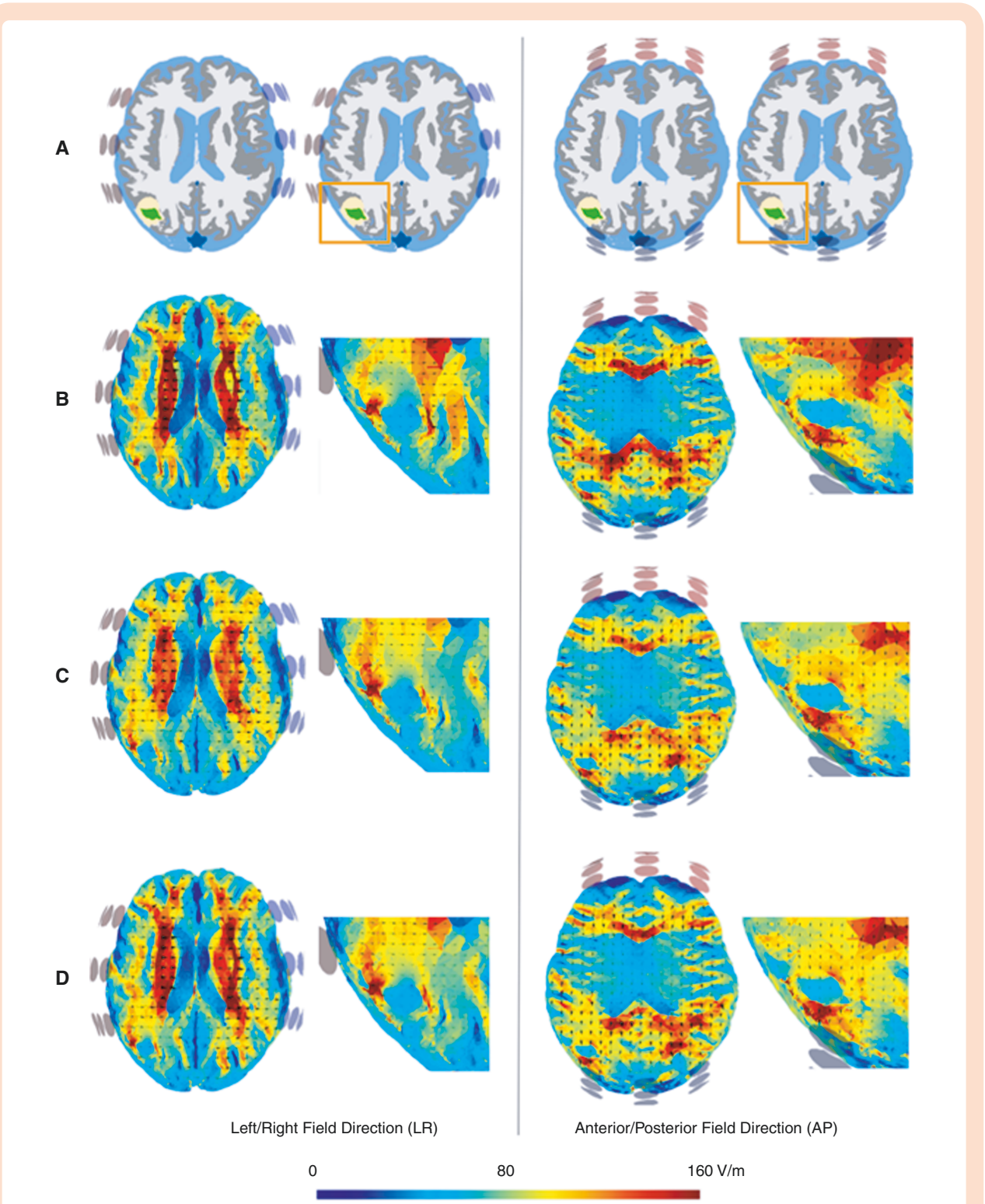

Figure 5. Comparison of electric fields generated using different conductivity properties of the brain tissue. The electrodes are displayed in an axial view, including the corpus callosum and brain tumor. The direction of the applied electric field is either left/right (LR) or anterior/posterior (AP), as depicted in the 2 columns respectively. (A) "Electrode Placement and Brain Anatomy" - The first row provides a view of the anatomical structures of the brain and the position of the electrodes. (B) "Isotropic Homogeneous Conductivities" - The electric field pattern when the brain tissue is assumed to have isotropic and homogeneous conductivities. The colors represent the field intensity, increasing from blue to red (V/cm). (C) "Isotropic Inhomogeneous Conductivities" - The distribution of the electric field assuming isotropic but inhomogeneous conductivities, calculated as the mean conductivities of the tensors from the direct mapping approach. (D) "Anisotropic Inhomogeneous Conductivities"—The electric field distribution with conductivities that are both inhomogeneous and direction-dependent (anisotropic), obtained directly from mapping. The arrows in the figure indicate the direction of the applied electric field, and a reference color scale is also provided for easy interpretation of field intensities.

principles of conductivity also affect tumor field intensity. Specifically, solid tumors with low-conductivity exhibit high field intensities, while high-conductivity tumor regions, such as central necrotic core(s) or surrounding edematous regions, will exhibit low field intensities.[39] As GBM is quite heterogeneous with necrotic regions, edema, and solid areas, it will typically exhibit a heterogeneous conductivity distribution and hence also field distribution. The necrotic core, which often consists of liquified cellular debris, may influence the electric field distribution at the adjacent tumor tissue, although this also depends on the conductivity of the adjacent tumor tissue.[36] Additionally, tumor morphology may have profound clinical implications in terms of TTFields distribution at the tumor site. When examining the field distribution of tumors that were purposefully shaped as classic geometric solids such as cube, cylinder, sphere, icosahedron, and cone it was observed that symmetric, less angulated geometries had generally lower electric fields. This is because electric charges tend to congregate near sharp or cornered spaces as opposed to smooth and rounded surfaces according to Coulomb's Law. Tumors with rounder surfaces may thus give rise to display more evenly distributed fields, while tumors exhibiting sharp surface edges may display higher field intensity. Therefore, it is suspected that patients with tumors displaying more irregular surfaces may experience increases in overall TTFields intensity.[36]

How Electric Field Distribution can be Modified to Benefit Patients

The "Edge Effect"

Since all transducers in a single array are connected to the same power source, higher electric field intensities, and current densities are observed at the edges of the outer transducers. This effect is called the "edge effect" (Figure 6) and is also known in other stimulation technologies such as tDCS. InTTFields therapy, the central transducer delivers the lowest current.[35] This is important in modeling studies and each pair of arrays should be modeled as connected to the same, shared current source to mimic the clinical setup. Most importantly, the "edge effect" should be considered when positioning the arrays for clinical treatment, as more effective treatment with higher field intensity can be expected if the edges of an array from either pair are placed in the vicinity of the tumor.

Transducer Array Positioning

Computational studies have examined the impact of array positioning on the median tumor field intensity and concluded that individualized electrode array placement significantly increases tumor field intensity by up to ~20% compared to the A/P and L/R position[35,40] as shown in Figure 7A. This observation was mainly due to the "edge effect."

In addition, it is an advantage when paired arrays are placed far apart. Studies have shown that moving the arrays closer together eg, towards the top of the head, will increase shunting of current through the scalp between the arrays, and hence reduce current flow to the brain and tumor. In the most extreme case of neighboring arrays, all energy will be disposed in the scalp with no antitumor effect as shown in Figure 7C.[41]

Furthermore, minor adjustments in the positioning of the electrode array are needed during treatment to avoid skin damage. These minor adjustments do not significantly affect the field distribution[40–42] as shown in Figure 7B, where rotating the transducer array stepwise from 0°C to 150°C with 30°C increments around its own axis does not significantly affect the field intensity. Figure 7 also shows that moving the transducer slightly (<3 cm)[41] in any direction from the optimal location does not significantly reduce field intensity.[41]

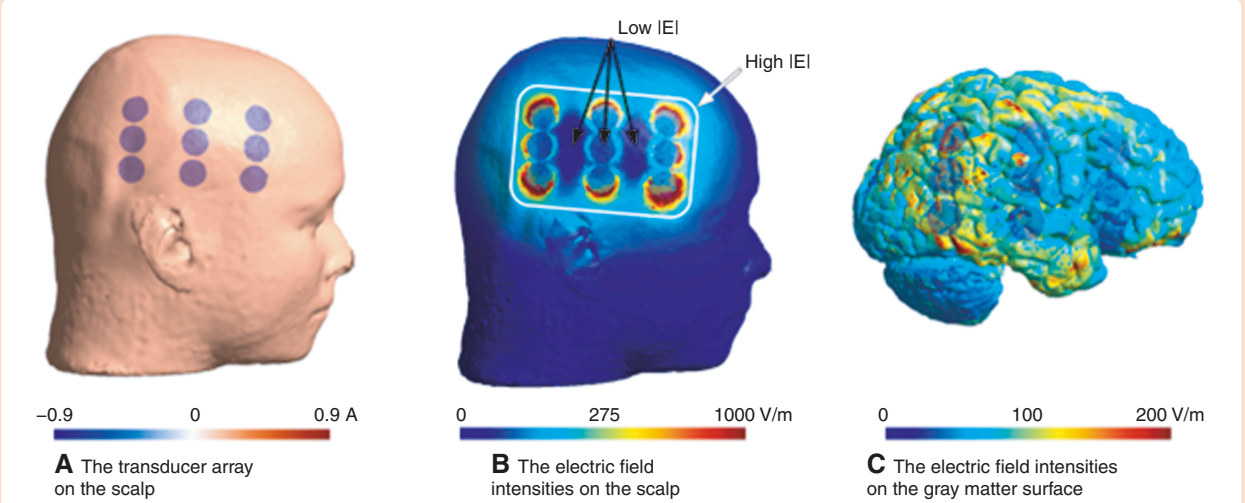

Figure 6. A single electrode array is shown in figure (A–C) shows the corresponding electric field intensity, which is highest around the edges and lowest in the center illustrating the "edge effect." Color-coded field intensity map in V/m. For example, a tumor located directly underneath the center electrode would experience lower field intensities and the transducer array could be moved accordingly so that the edges of the transducer arrays overlap the pathology for maximum field intensity.

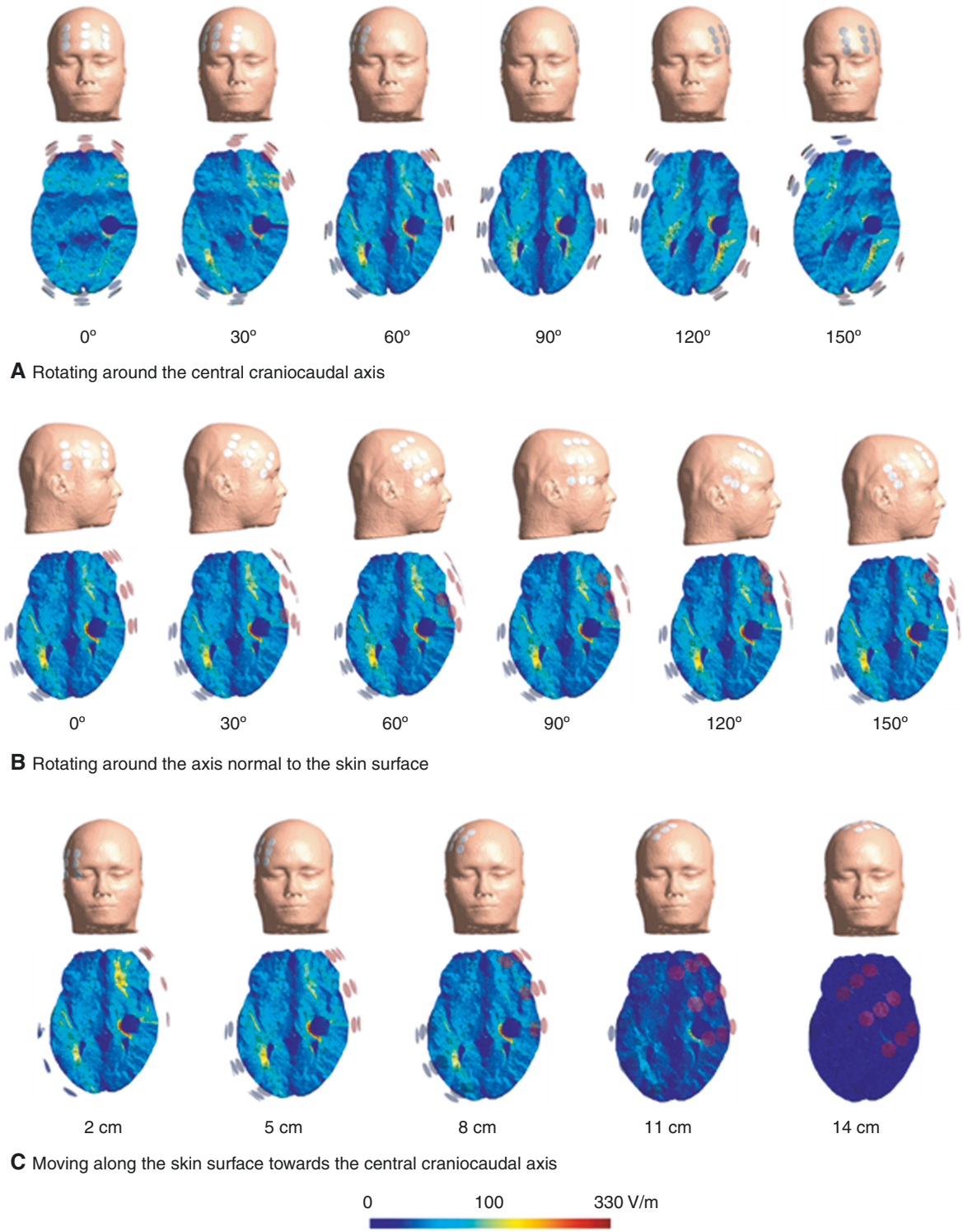

Figure 7. The computational head model is shown in Figure 3A. The transducer arrays are shown in white and gray. The model is color-coded, showing field intensity in V/cm. The lowest values are dark blue and highest are orange to red. (A) Arrays are rotated around the craniocaudal axis stepwise from 0 to 150 with 30-degree intervals. For each corresponding electrode array layout, the field strength is shown in the pathological area. Oblique array position produces higher field intensities in the tumor due to the "edge effect" and the lowest field intensities are seen in the standard anterior-posterior position depicted as 0°C. (B) A 30-degree stepwise rotation of the ipsilateral array around the axis normal to the skin surface at the center of the array located above the tumor. The contralateral array is maintained in the opposing position without rotation. The initial position is the same as the 60-degree position in (A). The rotation of the array does not affect the field strength significantly, which indicates that minor adjustments do not affect field strength. (C) A 1-cm stepwise movement of the array pair along the skin surface toward the central craniocaudal axis. The starting position of the array pair is 3 cm inferior to the 60-degree position in (A). This corresponds to 2, 5, 8, 11, and 14 cm on the skin surface toward the central craniocaudal z-axis. As the arrays are moved closer to the vertex of the head, the field intensity is diminished. When both arrays are at the top, the field intensity is close to zero due to shunting via the skin.

Infratentorial Tumors

The effect of TTFields on infratentorial GBM is unknown as the EF-14 trial[1] excluded this subgroup of patients. However, for infratentorial tumors including brainstem gliomas, computational studies have shown that the current array layout is subtherapeutic, and personalized electrode layouts involving new transducer array placements at the lower occipital and upper cervical region junction are superior and above the therapeutic threshold with >95% of the infratentorial averaged 1.7 V/cm and 2 V/cm for vertical and horizontal field direction, respectively, with a maximum of 2.8 V/cm.[43,44]

Other novel methods have been proposed to address the challenge of treating deeply seated and infratentorial tumors. A computational study revealed that field intensity was higher when arrays are surgically implanted directly at the location of the tumor.[45] Based on these results, another study examined endoscopic endonasal implantation of a flexible TTF-generating electrode array in the clivus as a novel treatment method for pediatric diffuse intrinsic pontine glioma.[46] These 2 studies demonstrated the potential benefit of alternative placing of arrays, but more research is needed to determine risks and benefits.

Field Enhancement With Skull-Remodeling Surgery

Skull-remodeling surgery (SR-surgery) was introduced to increase TTFields intensity in the region of interest. By surgically creating burr holes, craniectomies, or skull-thinning procedures, the low-conductive skull is removed to create high-conductive pathways for the electric current to flow into the tumor. Computational studies indicate that SR-surgery significantly increases the electric field strength in superficial tumors (30%–100%) with a minimal effect on WM and gray matter.[41,47–49]

The highest field enhancement was observed when SR surgery was performed directly above the tumor with the transducer arrays overlapping the skull defect, thus using the "edge effect."[41] Furthermore, a higher field enhancement was observed with several small burr holes compared with one craniectomy with same defect surface area.[47,48]

SR surgery was recently evaluated in a safety and feasibility study for rGBM. The study concluded that SR surgery in combination with TTFields therapy was safe and probably effective. The median OS was 15.5 months compared with the approximately 8.2 months in comparable population,[50] indicating a potential dose–response relationship. An ongoing randomized clinical phase II trial investigates the efficacy of SR-surgery.[51]

Heat and Thermal Modeling

The electric current flow induced by TTFields results in a temperature increase in the affected tissues, which may affect patients comfort, safety, and efficacy of the treatment.[52–57]

To ensure safety, each electrode, except the central one, has a thermistor to monitor scalp temperature.[58] The electric current is adjusted to keep the scalp temperature at a maximum of 39.5°C. Variations in the injected current lead to changes in the electric field in the tumor, altering the dose predicted through computational simulations.

The importance of heat modeling is described by Gentilal et al.[55,57] They found that the current injected in arrays placed <1 cm apart might be reduced due to the development of temperature hotspots secondary to the "edge effect," which could significantly reduce treatment response. These findings suggest that the array pairs should preferably be best placed as far from each other as possible to minimize heating between the arrays.

Computational work indicates that when the maximum scalp temperature is 39.5°C, which is the temperature that optimizes current injection, skull temperature is around 39.4°C and CSF is around 38°C, the temperature on the surface of the brain is increased with ≤0.1°C.[54] These values are below the thresholds reported in the literature, and no unexpected physiological changes were reported when applying TTFields therapy.[59] These computational studies indicate that TTFields therapy is safe for the patient from a thermal point of view, although long-term consequences of the impact of heat are uncertain.

Discussion and Future Perspectives

Computational modeling has been important in elucidating the MoA in TTFields therapy. Simulation studies have shown that the electric field distribution is shaped by specific anatomical features of the head and brain,[60] suggesting a need for individualized head modeling in patients undergoing TTFields therapy. However, it is difficult and time-consuming to create individualized head models, and fast and automatic methods would benefit research substantially.

The accuracy of computational studies depends on the assigned electric properties of tissues and often an isotropic conductivity is assumed[20,21,41,60] based on current data. Despite uncertainties associated with the reported conductivity, the simulated and measured fields corresponded reasonably well[61,62] with a discrepancy below 10%.[15] Individualized estimation of the conductive values using DTI[30,31] and wEPT[29] may potentially create more accurate models. However, more research is needed to validate these techniques and account for patient heterogeneity.

The general principles derived from computational studies can promote understanding of optimal dose distribution of applied TTFields in individual patients. Individualized transducer array placement using the "edge effect" may be considered when positioning the arrays for treatment, as the treatment effect is expected to be higher if the edges of an array from either pair are placed in the vicinity of the tumor.[35] However, placing the arrays within 1 cm of each other may increase the scalp temperature above the optimal threshold of 39.5°C. This leads to a lower injected current until scalp temperature is below threshold level,[55] which may eliminate benefits of the "edge effect." Therefore, when using the "edge effect" to create optimal tumor current flow, the arrays should preferably be placed at least 1 cm apart. Further research is needed on implications of the "edge effect" and variations in the injected current based on scalp temperature.

Furthermore, minor adjustments to array placement should be encouraged to avoid damage to the skin, which may potentially reduce treatment compliance. These minor adjustments will not affect dosimetry significantly.[41] Efficacy of TTFields therapy can be improved by adhering to a minimum patient compliance of at least 18 hours per day and minimizing overheating by no exposure to sun and use of appropriate headwear. Although the post hoc and subgroup analyses demonstrated a positive association between dose parameters and improved OS[18,19,23] future prospective multivariate analyses will help to determine the magnitude of this benefit when factors such as MGMT status, age, extent of resection, KPS, tumor size, cerebral edema, neurological deficits, and corticosteroid use are taken into account.

Nevertheless, these positive associations between patient compliance to TTFields therapy and improved OS[18] concluded a new expanded definition for TTFields dose as LMiDD. LMiDD is defined as the product of PLD and the average patient compliance during the first 6 months of therapy. LMiDD provides a single unifying value considering the 2 most important contributors of TTFields efficacy, (1) dose and (2) patient compliance. This approach is superior to retrospectively comparing single static dose metrics to prespecified compliance intervals. Thus, LMiDD is currently the best clinically validated dose measure.

Most patients with GBM still experience recurrence after TTFields therapy. Further research is thus needed to elucidate the exact mechanisms of TTFields and to develop a method to maximize TTFields therapy at the region of the highest risk of recurrence. A first step is to develop a Novotal 2.0 software tool that allows clinicians to perform similar dosimetry calculations as reported in previous studies.[23,24] This software tool must allow for (1) segmentation of normal and abnormal structures on patient's MRI scans, (2) delineation of TTFields dose distributions, and (3) fusion of prospective MRI scans to accurately identify and calculate TTFields dose distributions in areas of recurrence. The next step is to develop means to enhance the antimitotic and/or immune modulatory effects of TTFields either through direct manipulation of dose distribution or in combination with radiation therapy or systemic drug treatment.

Conclusion

This paper outlines the methodology and conclusions of existing computational head modeling and the potential benefits for patients undergoing TTFields therapy.

Evidence indicates that TTFields dose correlates with improved OS in patients with GBM and that areas of high dose are less likely to be the site of topographical recurrence. The dose depends on patient compliance, head anatomy, tumor size, location and morphology, tumor growth and peritumoral edema, electrode array position, the "edge effect," overheating of skin, and SR surgery.

However, more research on how to improve efficacy of TTFields therapy and thus OS in this patient group is highly warranted.

Supplementary material

Supplementary material is available online at *Neuro-Oncology* (https://academic.oup.com/neuro-oncology).

Funding

No funding was provided for this study.

Conflicts of interest statement

ARK is PI and NM is CI of a clinical trial (NCT04223999) partly funded by Novocure. Within the last 3 years, PCM has had research agreements with Novocure. For the last 3 years, NG has held research grants funded by Novocure
MB is offering consulting services for Zai Lab Ltd. ETW is the site PI for clinical trial NCT04471844 and PI for NCT04129515, both funded by Novocure
MG reports honoraria from Roche, Novartis, UCB, AbbVie, Daiichi Sankyo, Novocure, Bayer, Janssen-Cilag, Medac, Merck, Kyowa Kirin, Servier, CeCava, travel support from Novocure and Medac, and research grant from Novocure.

Authorship statement

Conception/Design: All Authors. Data collection/analysis: FC, AT, NM, and ARK. Statistical analysis: FC, AT. First draft of the manuscript: NM and ARK. Manuscript editing and critical revision: All authors. Supervision: ARK, AT, PCM, ETW, MB and MG. Creation of figures: FC, AT, ETW, NM, and ARK. Final approval of manuscript: All authors.

Affiliations

Department of Neurosurgery, Aarhus University Hospital, Aarhus, Denmark (N.M., A-D.R.K.); Department of Clinical Medicine, Aarhus University, Aarhus, Denmark (N.M., A-D.R.K.); Instituto de Biofísica e Engenharia Biomédica, Faculdade de Ciências da Universidade de Lisboa, Lisboa, Portugal (N.G., P.C.M.); Department of Health Technology, Center for Magnetic Resonance, Technical University of Denmark, Kgs. Lyngby, Denmark (F.C., A.T.); Danish Research Centre for Magnetic Resonance, Centre for Functional and Diagnostic Imaging and Research, Copenhagen University Hospital Amager and Hvidovre, Hvidovre, Denmark (F.C., A.T.); Brain Tumor Center and Neuro-Oncology Unit, Beth Israel Deaconess Medical Center, Boston, Massachusetts, USA (E.L.); Division of Hematology/Oncology, Department of Medicine, Rhode Island Hospital, Providence, Rhode Island, USA (E.T.W.); Department of Radiation Oncology, West Cancer Center and Research Institute, Memphis, Tennessee, USA (M.B.); Division of Clinical Neurooncology, Department of Neurology and German Cancer

Consortium (DKTK) Partner Site, University Hospital Essen, University Duisburg-Essen, Essen, Germany (M.G.)

References

1. Stupp R, Taillibert S, Kanner A, et al. Effect of tumor-treating fields plus maintenance temozolomide vs maintenance temozolomide alone on survival in patients with glioblastoma: A randomized clinical trial. *JAMA*. 2017; 318(23):2306–2316.
2. Moser JC, Salvador E, Deniz K, et al. The mechanisms of action of tumor treating fields. *Cancer Res*. 2022; 82(20):3650–3658.
3. Taphoorn MJB, Dirven L, Kanner AA, et al. Influence of treatment with tumor-treating fields on health-related quality of life of patients with newly diagnosed glioblastoma: a secondary analysis of a randomized clinical trial. *JAMA Oncol*. 2018; 4(4):495–504.
4. Stupp R, Wong ET, Kanner AA, et al. NovoTTF-100A versus physician's choice chemotherapy in recurrent glioblastoma: A randomised phase III trial of a novel treatment modality. *Eur J Cancer*. 2012; 48(14):2192–2202.
5. Wong ET, Lok E, Gautam S, Swanson KD. Dexamethasone exerts profound immunologic interference on treatment efficacy for recurrent glioblastoma. *Br J Cancer*. 2015; 113(2):232–241.
6. Wong ET, Swanson KD. Dexamethasone-friend or foe for patients with glioblastoma? *JAMA Neurol*. 2019; 76(3):247–248.
7. Regev O, Merkin V, Blumenthal DT, Melamed I, Kaisman-Elbaz T. Tumor-Treating Fields for the treatment of glioblastoma: A systematic review and meta-analysis. *Neurooncol Pract*. 2021; 8(4):426–440.
8. Ceresoli GL, Aerts JG, Dziadziuszko R, et al. Tumour Treating Fields in combination with pemetrexed and cisplatin or carboplatin as first-line treatment for unresectable malignant pleural mesothelioma (STELLAR): A multicentre, single-arm phase 2 trial. *Lancet Oncol*. 2019; 20(12):1702–1709.
9. Pless M, Droege C, von Moos R, Salzberg M, Betticher D. A phase I/II trial of Tumor Treating Fields (TTFields) therapy in combination with pemetrexed for advanced non-small cell lung cancer. *Lung Cancer*. 2013; 81(3):445–450.
10. Benavides M, Guillen C, Rivera F, et al. A phase II study of TTFields (150 kHz) concomitant with standard chemotherapy for front-line therapy of advanced pancreatic adenocarcinoma—Updated efficacy results. *J Clin Oncol*. 2017; 35(15_suppl):e15790–e15790.
11. Vergote I, von Moos R, Manso L, et al. Tumor Treating Fields in combination with paclitaxel in recurrent ovarian carcinoma: Results of the INNOVATE pilot study. *Gynecol Oncol*. 2018; 150(3):471–477.
12. Gkika E, Grosu AL, Macarulla Mercade T, et al. Tumor treating fields concomitant with sorafenib in advanced hepatocellular cancer: Results of the HEPANOVA phase II study. *Cancers (Basel)*. 2022; 14(6):1568.
13. Leal T, Kotecha R, Ramlau R, et al; LUNAR Study Investigators. Tumor Treating Fields therapy with standard systemic therapy versus standard systemic therapy alone in metastatic non-small-cell lung cancer following progression on or after platinum-based therapy (LUNAR): A randomised, open-label, pivotal phase 3 study. *Lancet Oncol*. 2023; 24(9):1002–1017.
14. Kirson ED, Gurvich Z, Schneiderman R, et al. Disruption of cancer cell replication by alternating electric fields. *Cancer Res*. 2004; 64(9):3288–3295.
15. Kirson ED, Dbalý V, Tovarys F, et al. Alternating electric fields arrest cell proliferation in animal tumor models and human brain tumors. *Proc Natl Acad Sci U S A*. 2007; 104(24):10152–10157.
16. Giladi M, Schneiderman RS, Voloshin T, et al. Mitotic spindle disruption by alternating electric fields leads to improper chromosome segregation and mitotic catastrophe in cancer cells. *Sci Rep*. 2015; 5:18046.
17. Porat Y, Giladi M, Schneiderman RS, et al. Determining the optimal inhibitory frequency for cancerous cells using Tumor Treating Fields (TTFields). *J Vis Exp*. 2017;18(123).
18. Toms SA, Kim CY, Nicholas G, Ram Z. Increased compliance with tumor treating fields therapy is prognostic for improved survival in the treatment of glioblastoma: A subgroup analysis of the EF-14 phase III trial. *J Neurooncol*. 2019; 141(2):467–473.
19. Kanner AA, Wong ET, Villano JL, Ram Z; EF-11 Investigators. Post Hoc analyses of intention-to-treat population in phase III comparison of NovoTTF-100A™ system versus best physician's choice chemotherapy. *Semin Oncol*. 2014; 41(suppl 6):S25–S34.
20. Wenger C, Salvador R, Basser PJ, Miranda PC. The electric field distribution in the brain during TTFields therapy and its dependence on tissue dielectric properties and anatomy: A computational study. *Phys Med Biol*. 2015; 60(18):7339–7357.
21. Miranda PC, Mekonnen A, Salvador R, Basser PJ. Predicting the electric field distribution in the brain for the treatment of glioblastoma. *Phys Med Biol*. 2014; 59(15):4137–4147.
22. Chaudhry A, Benson L, Varshaver M, et al. NovoTTF™-100A System (Tumor Treating Fields) transducer array layout planning for glioblastoma: A NovoTAL™ system user study. *World J Surg Oncol*. 2015; 13:316.
23. Ballo MT, Urman N, Lavy-Shahaf G, et al. Correlation of tumor treating fields dosimetry to survival outcomes in newly diagnosed glioblastoma: A large-scale numerical simulation-based analysis of data from the phase 3 EF-14 randomized trial. *Int J Radiat Oncol Biol Phys*. 2019; 104(5):1106–1113.
24. Glas M, Ballo MT, Bomzon Z, et al. The impact of tumor treating fields on glioblastoma progression patterns. *Int J Radiat Oncol Biol Phys*. 2021; 112(5):1269–1278.
25. Thielscher A, Antunes A, Saturnino GB. Field modeling for transcranial magnetic stimulation: a useful tool to understand the physiological effects of TMS? 2015 37th Annual International Conference of the IEEE Engineering in Medicine and Biology Society (EMBC). 2015:222–225.
26. Saturnino GB, Puonti O, Nielsen JD, Antonenko D, Madsen KH, Thielscher A. SimNIBS 2.1: a comprehensive pipeline for individualized electric field modelling for transcranial brain stimulation. In: Makarov S, Horner M, Noetscher G, eds. *Brain and Human Body Modeling: Computational Human Modeling at EMBC 2018*. Cham (CH): Springer.
27. Agn M, Munck Af Rosenschöld P, Puonti O, et al. A modality-adaptive method for segmenting brain tumors and organs-at-risk in radiation therapy planning. *Med Image Anal*. 2019; 54:220–237.
28. Puonti O, Van Leemput K, Saturnino GB, et al. Accurate and robust whole-head segmentation from magnetic resonance images for individualized head modeling. *Neuroimage*. 2020; 219:117044.
29. Wenger C, Hershkovich HS, Tempel-Brami C, Giladi M, Bomzon Z. Water-Content Electrical Property Tomography (wEPT) for mapping brain tissue conductivity in the 200–1000 kHz range: results of an animal study. In: Makarov S, Horner M, Noetscher G, eds. *Brain and Human Body Modeling: Computational Human Modeling at EMBC 2018*. Cham (CH): Springer.
30. Basser PJ, Mattiello J, LeBihan D. MR diffusion tensor spectroscopy and imaging. *Biophys J*. 1994; 66(1):259–267.
31. Basser PJ, Mattiello J, Lebihan D. Estimation of the effective self-diffusion tensor from the NMR spin echo. *J Magn Reson B*. 1994; 103(3):247–254.
32. Tuch DS, Wedeen VJ, Dale AM, George JS, Belliveau JW. Conductivity tensor mapping of the human brain using diffusion tensor MRI. *Proc Natl Acad Sci U S A*. 2001; 98(20):11697–11701.

33. Proescholdt M, Haj A, Doenitz C, et al. CBMT-14. The dielectric properties of brain tumor tissue. *Neuro Oncol.* 2019; 21(suppl 6):vivi35–vivi36.
34. Korshoej AR, Hansen FL, Thielscher A, von Oettingen GB, Sørensen JCH. Impact of tumor position, conductivity distribution and tissue homogeneity on the distribution of tumor treating fields in a human brain: A computer modeling study. *PLoS One.* 2017; 12(6):e0179214.
35. Korshoej AR, Hansen FL, Mikic N, et al. Importance of electrode position for the distribution of tumor treating fields (TTFields) in a human brain. Identification of effective layouts through systematic analysis of array positions for multiple tumor locations. *PLoS One.* 2018; 13(8):e0201957.
36. Lok E, San P, Hua V, Phung M, Wong ET. Analysis of physical characteristics of Tumor Treating Fields for human glioblastoma. *Cancer Med.* 2017; 6(6):1286–1300.
37. Lang ST, Gan LS, McLennan C, Monchi O, Kelly JJP. Impact of peritumoral edema during tumor treatment field therapy: A computational modelling study. *IEEE Trans Biomed Eng.* 2020; 67(12):3327–3338.
38. Lok E, Clark M, Liang O, et al. Modulation of tumor treating fields by cerebral edema from brain tumors. *Adv Radiat Oncol.* 2022; 101046(8).
39. Lok E, Clark M, Liang O, et al. Modulation of tumor-treating fields by cerebral edema from brain tumors. *Adv Radiat Oncol.* 2023; 8(1):101046.
40. Wenger C, Salvador R, Basser PJ, Miranda PC. Improving tumor treating fields treatment efficacy in patients with glioblastoma using personalized array layouts. *Int J Radiat Oncol Biol Phys.* 2016; 94(5):1137–1143.
41. Cao F, Mikic N, Wong ET, Thielscher A, Korshoej AR. Guidelines for burr hole surgery in combination with tumor treating fields for glioblastoma: A computational study on dose optimization and array layout planning. *Front Hum Neurosci.* 2022; 16:909652.
42. Macedo M, Wenger C, Salvador R, Fernandes SR, Miranda PC. Investigating an alternative ring design of transducer arrays for tumor treating fields (TTFields). *Annu Int Conf IEEE Eng Med Biol Soc.* 2016; 2016:5168–5171.
43. Lok E, San P, Liang O, White V, Wong ET. Finite element analysis of Tumor Treating Fields in a patient with posterior fossa glioblastoma. *J Neurooncol.* 2020; 147(1):125–133.
44. Ramirez-Fort MK, Naveh A, McClelland S, 3rd, et al. Computational simulations establish a novel transducer array placement arrangement that extends delivery of therapeutic TTFields to the infratentorium of patients with brainstem gliomas. *Rep Pract Oncol Radiother.* 2021; 26(6):1045–1050.
45. Segar DJ, Bernstock JD, Arnaout O, et al. Modeling of intracranial tumor treating fields for the treatment of complex high-grade gliomas. *Sci Rep.* 2023; 13(1):1636.
46. Ibn Essayed W, Jarvis CA, Bernstock JD, et al. Positioning transclival tumor-treating fields for the treatment of diffuse intrinsic pontine gliomas. *Life (Basel).* 2023; 13(3):601.
47. Korshoej AR, Saturnino GB, Rasmussen LK, et al. Enhancing predicted efficacy of tumor treating fields therapy of glioblastoma using targeted surgical craniectomy: A computer modeling study. *PLoS One.* 2016; 11(10):e0164051.
48. Yang X, Liu P, Xing H, et al. Skull modulated strategies to intensify tumor treating fields on brain tumor: A finite element study. *Biomech Model Mechanobiol.* 2022; 21(4):1133–1144.
49. Jin T, Dou Z, Zhao Y, et al. Skull defect increases the tumor treating fields strength without detrimental thermogenic effect: A computational simulating research. *Cancer Med.* 2023; 12(2):1461–1470.
50. Werlenius K, Kinhult S, Solheim TS, et al. Effect of disulfiram and copper plus chemotherapy vs chemotherapy alone on survival in patients with recurrent glioblastoma: A randomized clinical trial. *JAMA Netw Open.* 2023; 6(3):e234149–e234149.
51. Mikic N, Poulsen FR, Kristoffersen KB, et al. Study protocol for OptimalTTF-2: enhancing Tumor Treating Fields with skull remodeling surgery for first recurrence glioblastoma: A phase 2, multi-center, randomized, prospective, interventional trial. *BMC Cancer.* 2021; 21(1):1010.
52. Gentilal N, Salvador R, Miranda PC. Temperature control in TTFields therapy of GBM: Impact on the duty cycle and tissue temperature. *Phys Med Biol.* 2019; 64(22):225008.
53. Gentilal N, Miranda PC. Heat transfer during TTFields treatment: influence of the uncertainty of the electric and thermal parameters on the predicted temperature distribution. *Comput Methods Programs Biomed.* 2020; 196:105706.
54. Gentilal N, Abend E, Naveh A, et al. Temperature and impedance variations during tumor Treating Fields (TTFields) Treatment. *Front Hum Neurosci.* 2022; 16:931818.
55. Gentilal N, Naveh A, Marciano T, et al. A computational study of the relation between the power density in the tumor and the maximum temperature in the scalp during Tumor Treating Fields (TTFields) therapy. *Annu Int Conf IEEE Eng Med Biol Soc.* 2021; 2021:4192–4195.
56. Gentilal N, Salvador R, Miranda PC. A thermal study of tumor-treating fields for glioblastoma therapy. In: Makarov SN, Noetscher GM, Nummenmaa A, eds. Brain and Human Body Modeling 2020: Computational Human Models Presented at EMBC 2019 and the BRAIN Initiative® 2019 Meeting. Cham (CH): Springer.
57. Gentilal N, Naveh A, Marciano T, Miranda PC. The impact of Scalp's temperature on the choice of the best layout for TTFields Treatment. *IRBM.* 2023; 44(3):100768.
58. Wasserman Y, Krinitsky M, Shtotland, M, Kaikov, V. Temperature measurement in arrays for delivering TTFields. US2018. US20200269043A1.
59. Wang H, Wang B, Normoyle KP, et al. Brain temperature and its fundamental properties: A review for clinical neuroscientists. *Front Neurosci.* 2014; 8:307.
60. Opitz A, Paulus W, Will S, Antunes A, Thielscher A. Determinants of the electric field during transcranial direct current stimulation. *Neuroimage.* 2015; 109:140–150.
61. Huang Y, Liu AA, Lafon B, et al. Measurements and models of electric fields in the in vivo human brain during transcranial electric stimulation. *Elife.* 2017; 6:e18834.
62. Opitz A, Yeagle E, Thielscher A, et al. On the importance of precise electrode placement for targeted transcranial electric stimulation. *Neuroimage.* 2018; 181:560–567.